Discover Oncology

Research

Exploration of the mechanism of Polyphyllin I against hepatocellular carcinoma based on network pharmacology, molecular docking and experimental validation

Yilong Chen[1,2] · Qiuying Wang[3,4] · Shuixiu Bian[1,2] · Jing Dong[1,4] · Jie Xiong[5] · Jiamei Le[1,2]

Received: 14 October 2024 / Accepted: 8 April 2025
Published online: 28 May 2025

Abstract

Purpose Hepatocellular carcinoma (HCC) is a leading cause of cancer-related death worldwide. Targeted therapies hold promise for HCC treatment, and understanding the molecular mechanisms of action is crucial for developing novel therapeutic strategies. Polyphyllin I, a natural compound with known antitumor activity, represents a potential therapeutic candidate.

Methods This study employed a network pharmacology approach to investigate the anti-HCC effects of Polyphyllin I and its underlying mechanisms. Drug and disease related targets were identified and intersected to construct Components-Gene Symbols-Disease and Protein–Protein Interaction networks. Gene Ontology (GO) and Kyoto Encyclopedia of Genes and Genomes (KEGG) pathway enrichment analyses were performed. Molecular docking simulations were conducted to explore the interactions between Polyphyllin I and key pathway proteins (VEGF-C and β-catenin). Finally, in *vitro* and in *vivo* experiments validated the anti-HCC effects and underlying mechanisms of Polyphyllin I.

Results Network pharmacology analysis revealed that Polyphyllin I targets multiple genes and pathways implicated in HCC development and progression. GO and KEGG analyses identified significant enrichment of pathways related to cell proliferation, apoptosis and angiogenesis, including VEGF and the Wnt/β-catenin signaling pathways. Molecular docking simulations demonstrated strong binding affinities between Polyphyllin I and VEGF-C and β-catenin. In vitro and in vivo experiments confirmed that Polyphyllin I effectively inhibits HCC cell proliferation, induces apoptosis, and suppresses angiogenesis, potentially by modulating the VEGF-C and Wnt/β-catenin signaling pathways.

Conclusions The study provides compelling evidence for the antitumor activity of Polyphyllin I in HCC and elucidates its possible molecular mechanisms, suggesting that Polyphyllin I holds great potential as a therapeutic agent for HCC.

Keywords Hepatocellular carcinoma · Network pharmacology · Molecular docking · Polyphyllin I · VEGF-C · Wnt/β-catenin signaling pathway

Supplementary Information The online version contains supplementary material available at https://doi.org/10.1007/s12672-025-02341-5.

✉ Jie Xiong, doctorxiongj@163.com; ✉ Jiamei Le, lejm@sumhs.edu.cn | [1]Shanghai Key Laboratory of Molecular Imaging, Zhoupu Hospital, Shanghai University of Medicine and Health Sciences, Shanghai 201318, China. [2]School of Health Science and Engineering, University of Shanghai for Science and Technology, Shanghai 200093, China. [3]School of Chinese Materia Medica, Nanjing University of Chinese Medicine, Nanjing 210023, China. [4]School of Pharmacy, Shanghai University of Medicine and Health Sciences, Shanghai 201318, China. [5]Department of Gastroenterology and Hepatology, Tongji Hospital, Tongji University School of Medicine, Shanghai 200065, China.

Fig. 1 Flow chart of network pharmacology, molecular docking and experimental studies on the anti-hepatocellular carcinoma effect of ▶ Polyphyllin I. The process is mainly divided into two parts, the first part is the network pharmacology and molecular docking, and the second part is the in vivo and in vitro experimental verification

1 Introduction

Primary liver cancer was the sixth most frequently diagnosed cancer and the third leading cause of cancer-related mortality globally in 2020 [1, 2]. Hepatocellular carcinoma (HCC) is the predominant subtype of primary liver cancer worldwide, representing approximately 75–85% of all clinical cases [2]. Despite the availability of multiple treatment options, including liver transplantation, surgical resection, radiotherapy, chemotherapy, and immunotherapy, conventional therapies often face limitations such as high recurrence rates, severe side effects, and reduced efficacy in advanced disease [3, 4]. Although the FDA has approved several targeted therapies for hepatocellular carcinoma, such as sorafenib, lenvatinib, regorafenib, cabozantinib, and ramucirumab, these therapies have limitations, including insignificant efficacy, severe side effects, and the emergence of drug resistance [5–8]. These challenges highlight the urgent need for new, safer, and more targeted treatment strategies for HCC.

Traditional Chinese medicine (TCM), with its holistic approach and emphasis on individualized treatment, has long been used as a complementary and alternative approach for cancer treatment [9]. Numerous TCM herbs and formulations have shown promising anti-tumor activities with potentially fewer side effects compared to conventional therapies [10]. *Paris polyphylla* (Chinese name: Chonglou), a traditional Chinese medicine with a history of use for millennia in treating a range of conditions including bleeding, traumatic injuries, sores, and snake bites [11], has gained increasing attention for its potent anti-cancer properties [12]. Polyphyllin I (PPI), a key active ingredient of *Paris polyphylla*, has demonstrated promising antitumor activity in various cancers [11, 12], and a growing body of evidence supports its potential as a therapeutic agent for HCC.

Several studies have shown that PPI inhibits the growth of HCC in vivo and in vitro, induces apoptosis, and suppresses stem cell-like properties [13, 14]. Furthermore, research suggests that the in vivo therapeutic effect of a PPI dose of 8 mg/kg is comparable to that of a Sorafenib dose of 30 mg/kg, and that PPI may enhance the efficacy of existing HCC therapies (such as sorafenib) through synergistic mechanisms [13]. Notably, PPI has also demonstrated minimal host toxicity in preclinical studies [14]. While these preclinical studies provide a foundation for understanding PPI's anti-HCC effects, the precise molecular mechanisms by which it exerts these effects remain incompletely understood. Recent studies have highlighted various potential mechanisms, including inducing ferroptosis [15], modulating autophagy [16], affecting signaling pathways such as PPARγ/RXRα [14], AKT/GSK-3β/β-catenin [13], and VEGF-A [17]. However, a comprehensive understanding of these mechanisms and their interconnections is still lacking. Therefore, it is essential to further elucidate the specific mechanisms by which PPI exerts its anti-HCC effects.

Network pharmacology is an emerging field that integrates network analysis, systems biology, and computational chemistry to identify the mechanisms of action of drugs and their targets at a system level [18]. Unlike traditional drug discovery approaches, which focus on the identification of individual drug-target interactions, network pharmacology aims to understand the complex interactions between drugs, targets, pathways, and diseases in a holistic manner [19]. This approach can help to identify novel drug targets and therapeutic strategies, as well as to predict potential adverse effects and drug-drug interactions. In recent years, network pharmacology has been applied to the discovery and development of drugs for various diseases, including cancer [20]. By constructing and analyzing drug-target networks, researchers can identify the key nodes and pathways that are involved in the development and progression of cancer, as well as the mechanisms of action of anti-cancer drugs. In particular, network pharmacology can help to identify multi-target drugs that can modulate multiple signaling pathways simultaneously, thereby increasing their therapeutic efficacy and reducing the risk of drug resistance [21].

In this study, we used network pharmacology to explore the potential molecular mechanisms and pathways of PPI on HCC through visual analysis, utilizing various databases and computational tools. To further validate the prediction results obtained from the analysis, we performed molecular docking experiments on the predicted results. In addition, we conducted experiments in vitro and in vivo to verify the effects and potential mechanisms of PPI on HCC. It is expected that our research may help to clarify the mechanism and targets of PPI in the treatment of HCC. A schematic representation pertaining to the methodology employed in this research is illustrated in Fig. 1.

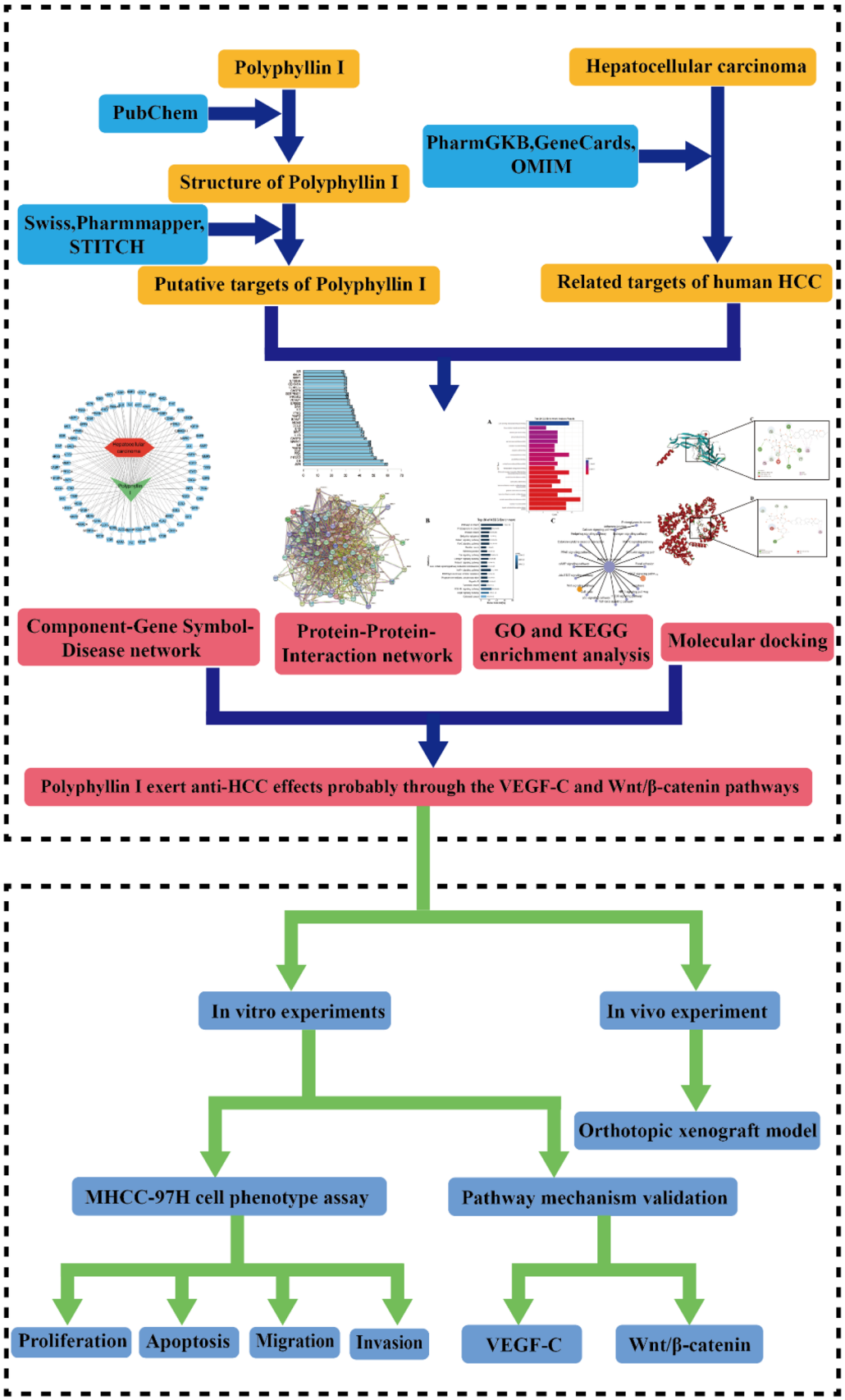
Polyphyllin I
PubChem
Structure of Polyphyllin I
Swiss,Pharmmapper, STITCH
Putative targets of Polyphyllin I
Hepatocellular carcinoma
PharmGKB,GeneCards, OMIM
Related targets of human HCC
Component-Gene Symbol-Disease network
Protein-Protein-Interaction network
GO and KEGG enrichment analysis
Molecular docking
Polyphyllin I exert anti-HCC effects probably through the VEGF-C and Wnt/β-catenin pathways
In vitro experiments
In vivo experiment
Orthotopic xenograft model
MHCC-97H cell phenotype assay
Pathway mechanism validation
Proliferation
Apoptosis
Migration
Invasion
VEGF-C
Wnt/β-catenin

2 Materials and methods

2.1 Collection of drug/disease-related targets

The structure of PPI was obtained from the PubChem database (https://pubchem.ncbi.nlm.nih.gov). The structure of PPI was uploaded to multiple databases to obtain their potential targets, including SwissTargetPrediction (http://www.swisstargetprediction.ch/), PharmMapper (http://lilab-ecust.cn/pharmmapper/submitfile.html), STITCH (https://stitch.embl.de/) [22–25]. Then, the term "Hepatocellular carcinoma" was searched in multiple databases, including GeneCards (http://www.genecards.org/), OMIM (http:/ www.omim.org/), and PharmGKB (https://www.pharmgkb.org/) [26–28]. A correlation score threshold > 10 was used to filter the extensive target information obtained from GeneCards for subsequent research. All targets were "Homo sapiens" and calibrated to uniform names through the Uniprot database (https://www.uniprot.org/) [29]. After removing the duplicated genes, related genes were returned. The intersection of the targets related to the drug and disease was obtained and drawn into a Venn diagram, which were the potential gene targets of PPI for the treatment of HCC.

2.2 Construction of pharmacology network and protein–protein interaction network

After extracting intersection targets, a Components-Gene Symbols-Disease(C-G-D) information network graph was constructed based on the interactions of drug components, gene targets and diseases. And the C-G-D network was visualized by Cytoscape 3.9.1 software [30]. Subsequently, the Gene Symbols for both HCC and PPI were entered into the STRING database (https://string-db.org/) to construct the Protein–Protein Interaction network [31]. To ensure the reliability of the results, the search was limited to Homo sapiens and a confidence score threshold of ≥ 0.4 was set.

2.3 Gene ontology (GO) and kyoto encyclopedia of genes and genomes (KEGG) pathway enrichment analyses

To prepare for the GO and KEGG enrichment analyses, Gene Symbols obtained from the previous step were converted into Entrez IDs using a Perl language script. The Bioconductor package (R) v3.16 (http://bioconductor.org/) was utilized for the GO analysis, which provides a comprehensive set of functional annotation tools to elucidate the biological significance behind a large number of genes [32]. KEGG analysis was conducted on the OmicShare website (https://www.omicshare.com/). A P-value of < 0.05 indicated statistical significance of the degree of enrichment. The results were then presented as bubble plots and bar graphs using the R language.

2.4 Molecular docking

Molecular docking was conducted to explore the interactions between the PPI and the potential targets. The 3D structures of VEGF-C and β-catenin were obtained from the RCSB-PDB database (https://www.rcsb.org/) in PDB format. The receptors were prepared by dehydration and hydrogenation in Discovery Studio 2019 software (V19.1), and subsequently, the PPI was subjected to molecular docking studies with the VEGF-C and β-catenin, respectively, using Discovery Studio software. Select Dock Ligands (LibDock) under Dock Ligands in Receptor-Ligand Interactions as the docking program. In the parameters, only change Max Hits to Save in Docking Preferences to 10, select Input Ligands as the PPI structure obtained from the PubChem website, and keep the other default values. Select Calculate Binding Energies under Dock Ligands in Receptor-Ligand Interactions as the docking free energy program, select PPI as Input Ligands in the parameters, and select In Situ Ligand Minimization and Ligand Conformational Entropy as True. Save the results after running. Finally, data analysis and mapping were carried out using Discovery Studio.

2.5 In vivo experiment in orthotopic xenograft model

Six-week-old male athymic BALB/c nude mice were procured from Beijing Vital River Laboratory Animal Technology Co., Ltd. (Beijing, China). The animals were housed in the animal house of Shanghai University of Medicine & Health Sciences under controlled conditions of temperature (20 ± 2 °C), humidity (60 ± 5%), and a 12-h light/dark cycle. MHCC-97H

luciferase cells (4×10^6) resuspended in 40 µL PBS/Matrigel (1:1) were inoculated under the left liver lobe envelope of the mice. After a week of tumor cells implantation (Day 0), the in situ transplanted tumor-bearing mice were randomly divided into two groups: PPI administration group (n = 5, intraperitoneal injection of 10 mg/kg/d, dissolved in 5% DMSO + 40% PEG300 + 5% Tween 80 + 50% deionized water), as described previously [17, 33], and model control group (n = 5, administered with an equal volume of vehicle). After anesthetizing the mice with isoflurane, tumor formation was monitored using the Xenogen In Vivo Imaging System (IVIS) (Caliper Life Sciences, Hopkinton, USA). After 14 days of treatment, mice were injected intraperitoneally with 4 mg of fluorescein (Gold Biotech) for 10 min. Then the mice were anesthetized with isoflurane, and the formation of metastasis and progression of tumor formation were monitored using the Xenogen IVIS. After euthanizing the mice through overdose of isoflurane inhalation, the livers were resected, photographed and weighed. Then all tumor nodules were carefully dissected from the liver and weighed, as previously described [34, 35]. Relative liver weight was calculated using the following formula:

$$\text{Relative liver weight} = (\text{liver weight}/\text{body weight}) \times 100\%.$$

The experimental procedures were approved by the Institutional Animal Care and Use Committee of Shanghai University of Medicine & Health Sciences.

2.6 Cell culture and reagents

The MHCC-97H human HCC cell line was acquired from the Cell Bank of Type Culture Collection of the Chinese Academy of Sciences (Shanghai, China) and cultured in Dulbecco's modified Eagle's medium (DMEM) containing 1% penicillin–streptomycin and 10% Fetal Bovine Serum (FBS) in a cell culture incubator (Thermo Fisher; USA) at 37℃ and 5% CO_2. The complete DMEM was replaced every other day. PPI was obtained from Selleck Chemicals (Shanghai, China) dissolved in DMSO for all cell assays. The DMEM, FBS, penicillin–streptomycin and Phosphate Buffered Saline (PBS) were purchased from Gibco (Carlsbad, CA, USA). Other reagents were purchased from Sigma-Aldrich (Shanghai, China) unless otherwise specified.

2.7 Cell viability assay

The CCK8 Kit (Dojindo Co. Ltd; Shanghai, China) was utilized to evaluate cell viability. Well-grown MHCC-97H cells were counted and seeded in a 96-well plate at a density of 2000 cells per well in 100 µL of cell suspension. Then the adherent cells were divided into six groups including blank, control, and PPI-treated groups with a series of concentrations (2.5, 5, 10, and 20 µM). After culturing for 24 h, the cells were incubated with 100 µL of DMEM containing 10% CCK8 detection solution for an additional 4 h. Finally, the OD value was determined at a wavelength of 450 nm using the microplate reader (Potenov; Beijing, China). The cell viability percentage was calculated using the following formula: Cell viability (%) = (OD of treatment − OD of blank) / (OD of control − OD of blank) × 100%.

2.8 Cell apoptosis assay

Well-grown MHCC-97H cells were seeded at 5×10^4/mL per well in 6-well plates. The adherent cells were then divided into 0, 1 and 2.5 µM PPI drug-treated groups. After 24 h of incubation, the cells were incubated with 10 µL Annexin V-FITC complex (Dojindo Co. Ltd; Shanghai, China) and PPI mixture for another 15 min at room temperature and in the dark. Finally, the apoptotic percentage of cells was analyzed by the flow cytometer (BD Biosciences; USA) and quantified using FlowJo 10.4 software.

2.9 Transwell assay

The matrigel coated transwell plates (354,480; Corning; USA) were used to detect the ability of invasion in MHCC-97H cells. Serum-free medium (200 µL) containing PPI solution at concentrations of 0, 1 and 2.5 µM was added to the upper chamber with 2×10^5 cells, and 600 µL DMEM was added to each well of the lower chamber. After incubating for 24 h, the cells on the bottom surface of the upper chamber were fixed for 20 min and then stained with 0.1% crystalline violet for 20 min. Finally, the cells were photographed and counted in 5 random fields under a 100 × inverted microscope (Leica Microsystems; Germany).

2.10 Wound healing scratch test

Ibidi culture inserts (Ibidi; Germany) were set onto 6-well plates. Then the MHCC-97H cells (9×10^4/mL) were inoculated into the well of Ibidi isolation chambers. After the cells had adhered to the wall and grown to 100% confluence, the Ibidi insert was gently removed, leaving an approximately 500 μm wide gap. Subsequently, the control and PPI-treated groups were treated by 0, 1, 2.5 μM PPI for 48 h. Finally, the images were taken after 0, 24 and 48 h incubation using the 100 × inverted microscope, and the rate of wound closure was measured by Image J software.

2.11 RT-qPCR assay

After treating MHCC-97H cells with PPI at 0 and 2.5 μM for 24 h, total RNA was extracted using a kit (TOYOBO Co., Ltd., Shanghai, China) according to the manufacturer's instructions. The total RNA concentrations were determined by using an ultra-micro spectrophotometer (DeNovix DS11, DE, USA). After the quality and concentrations of RNA were determined, cDNA was synthesized with the ReverTra Ace qPCR RT Kit (TOYOBO Co., Ltd., Shanghai, China) by following the protocol described by the manufacturer. After mixing 20 μL PCR reaction system, the PCR reaction was performed using ABI Prism TM 7500 Real-Time qPCR System (Applied Biosystems; Thermo Fisher Scientific, Inc.). The β-actin was used as a housekeeping gene to normalize the expression level of the test genes, and the relative gene expression level was analyzed using the $2^{-\Delta\Delta CT}$ method. All samples were analyzed in triplicate. Primers were synthesized by GENEWIZ (Suzhou, China). The primer sequences are listed below: β-actin: forward: 5′-GGGAAATCGTGCGTGACATTAAG-3′, reverse: 5′-TGTGTTGGCGTACAGGTCTTTG-3′; VEGF-C: forward: 5′-GCAGAATCATCACGAAGTGGT-3′, reverse: 5′-CCAGGGTCTCGATTGGATGG-3′; β-catenin: forward: 5′-GAAACAGCTCGTTGTACCGC-3′, reverse: 5′-ATCCACTGGTGAACCAAGCA-3′.

2.12 Western blot assay

MHCC-97H cells treated with PPI at 0 and 2.5 μM for 24 h were collected, lysed in RIPA lysis solution for 45 min in an ice bath at 12,000 r/min and centrifuged for 15 min at 4 °C. The protein concentration was determined by BCA with the supernatant protein lysis solution, added to 1 × loading buffer and boiled for 10 min in a metal water bath at 100 °C to denature the protein. After SDS-PAGE electrophoresis, the membranes were transferred to PVDF membranes and blocked by 5% BSA. The membranes were then incubated with primary antibodies: rabbit monoclonal antibodies against β-catenin, VEGF-C, GAPDH (diluted 1:1000; ABclonal Co., Ltd., Shanghai, China) in TBST containing 5% BSA at 4 °C overnight. The PVDF membrane was washed with TBST (Shanghai Epizyme Biomedical Technology Co., Ltd., Shanghai, China) and the HRP-conjugated anti-rabbit secondary antibody (diluted 1:10,000; ABclonal Co., Ltd., Shanghai, China) was incubated at room temperature for 2 h. The bands were detected using the enhanced chemiluminescence (ECL) system. Finally, the band intensity of proteins was quantified by using ImageJ software and the relative expression of protein was normalized by expression of GAPDH.

2.13 Statistical analysis

All measured data were presented as means ± SEM. Differences were assessed by using Student's t-test with 95% confidence level in two independent samples. Comparisons for more than two groups were evaluated using one-way ANOVA followed by POST HOC LSD. GraphPad Prism 8 was used for graphing. All statistical analyses were performed using SPSS 26.0 software. The statistical significance was defined as $P < 0.05$.

3 Results

3.1 The potential targets of PPI against HCC

Targets of PPI were obtained from three database websites. Firstly, "Polyphyllin I" was searched on the PubChem database website, and its Canonical SMILES and 2D structure were obtained (Fig. 2A). The 2D structure was uploaded to the PharmMapper database website to obtain 299 targets. A total of 13 targets were obtained by selecting targets

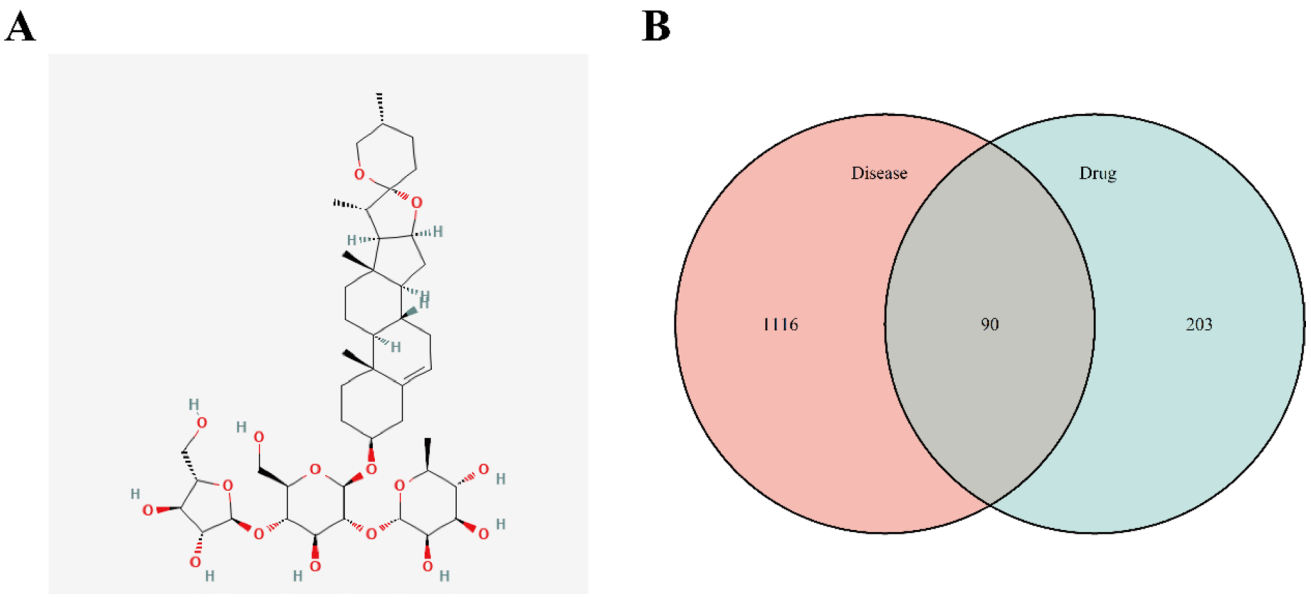

Fig. 2 PPI structures and intersection targets. **A** Chemical structure of PPI. **B** Number of HCC and PPI targets and the overlap between them. There are 1206 disease targets depicted in red on the left. The blue section on the right represents drug targets, amounting to 293 in total. There is an intersection of 90 targets between these two categories

with a Probability greater than 0 in Swiss Target Prediction.Only three targets were collected in the STITCH database and were duplicates of those found in the two previous databases. After removing duplicate genes, a total of 293 targets for PPI were obtained (Supplementary Table S1).

Targets related to HCC were obtained from three database websites. The GeneCards, OMIM, and PharmGKB database websites were searched for HCC, and 10,339, 49, and 14 targets related to HCC were obtained, respectively. In GeneCards, targets were selected with Relevance scores greater than 10, resulting in 1201 targets satisfying the condition. After removing duplicate genes, a total of 1206 HCC-related targets were obtained (Supplementary Table S2). To analyse the targets of PPI against HCC, we took the intersection of 1,206 HCC-associated targets and 293 PPI-associated targets, and obtained a total of 90 overlapping targets, as shown in Fig. 2B (Supplementary Table S3).

3.2 Analysis of effective components—gene symbols—disease network

Traditional Chinese medicines are known for their ability to act on numerous molecular targets. To investigate the potential mechanisms of PPI against HCC, we constructed a C-G-D network using Cytoscape software (Fig. 3). Among the 90 potential targets of PPI, there are targets related to cell proliferation, cell invasion and metastasis, such as EGFR, STAT3, MMP3, and apoptosis-related targets, such as CASP3 and CASP7. This network analysis suggests that PPI may exert its anti-HCC effect by simultaneously targeting multiple pathways that are critical for tumor growth, invasion and survival.

3.3 Protein–protein interaction network of PPI-related HCC targets

As shown in Fig. 4A, the Protein–Protein Interaction network consists of 95 nodes and 1194 edges (Supplementary Table S4). The Protein–Protein Interaction network provides insight into the molecular interactions and pathways involved in PPI-mediated HCC treatment. Nodes with higher scores in the Protein–Protein Interaction network may be more important in the pharmacological process, and the top 30 proteins may contain key molecular targets in PPI-mediated HCC, as illustrated in Fig. 4B. Specifically, JUN, IL6, PTGS2, FOS, EGF, MMP9, IL8, MAPK1, CASP3 and IL1B are the top 10 key proteins, which are associated with the cell growth, apoptosis and migration of tumor cells (Supplementary Table S5). It is suggested that PPI may inhibit tumor cell proliferation and migration and promote tumor cell apoptosis.

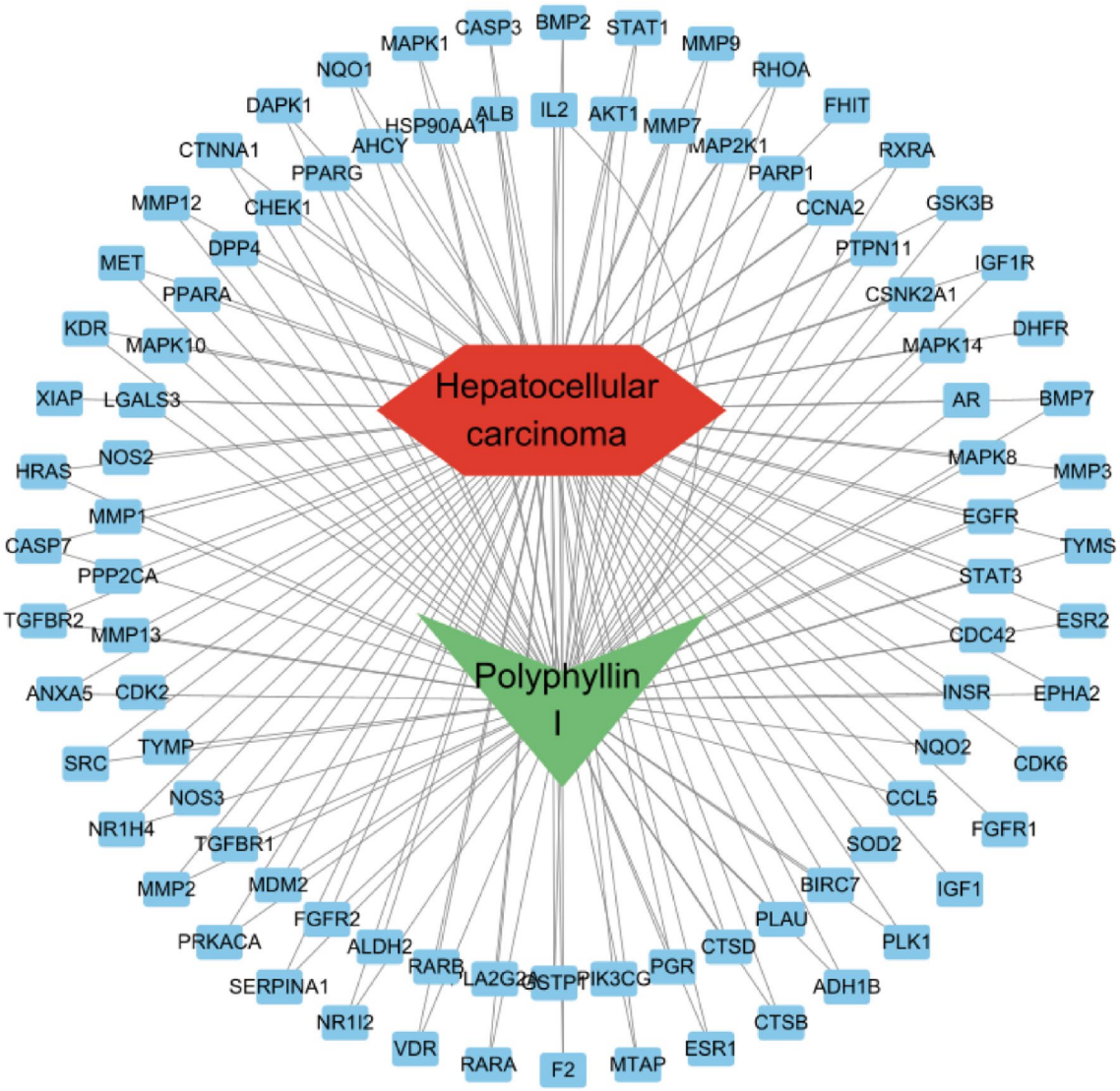

Fig. 3 Components-Gene Symbols-Disease (C-G-D) network. Green nodes represent PPI, red nodes indicate HCC, and blue nodes represent the overlapping gene symbols of PPI and HCC, while the edges indicate possible interactions between the nodes

3.4 GO enrichment and KEGG pathway analysis

To further elucidate the functions and mechanisms of PPI, we performed GO enrichment and KEGG pathway analyses on the 90 targets derived previously. As shown in Fig. 5A, GO enrichment analysis revealed that the most enriched terms were related to "Protein Serine/Threonine Kinase Activity", "Protein Serine Kinase Activity RNA Polymerase II-Specific", and "DNA-Binding Transcription Factor Binding" (Supplementary Table S6). These enriched GO terms highlight the potential roles of PPI in regulating crucial cellular processes such as signal transduction, gene expression, and transcription, which are often dysregulated in cancer. Subsequently, KEGG pathway analysis (Fig. 5B) identified the top enriched pathways as "Pathways in Cancer", "PIK3-AKT signaling pathway" and "Proteoglycans in Cancer" (Supplementary Table S7). Notably, "Pathways in Cancer" emerged as the most significantly enriched pathway, further emphasizing the potential anti-tumor effects of PPI. Given the significant enrichment of the "Pathways in Cancer", we further investigated its sub-pathways (Fig. 5C**)**. This analysis revealed the involvement of several crucial signaling pathways, including the PPAR Signaling Pathway, Wnt/β-catenin Signaling Pathway, and VEGF Signaling Pathway. The VEGF pathway is closely linked to tumorigenesis and cancer stem cell function, playing a crucial role in the pathogenesis of many cancers [36]. Similarly, the Wnt/β-catenin signaling pathway is known to be critically involved in the development and progression of various cancers [37].

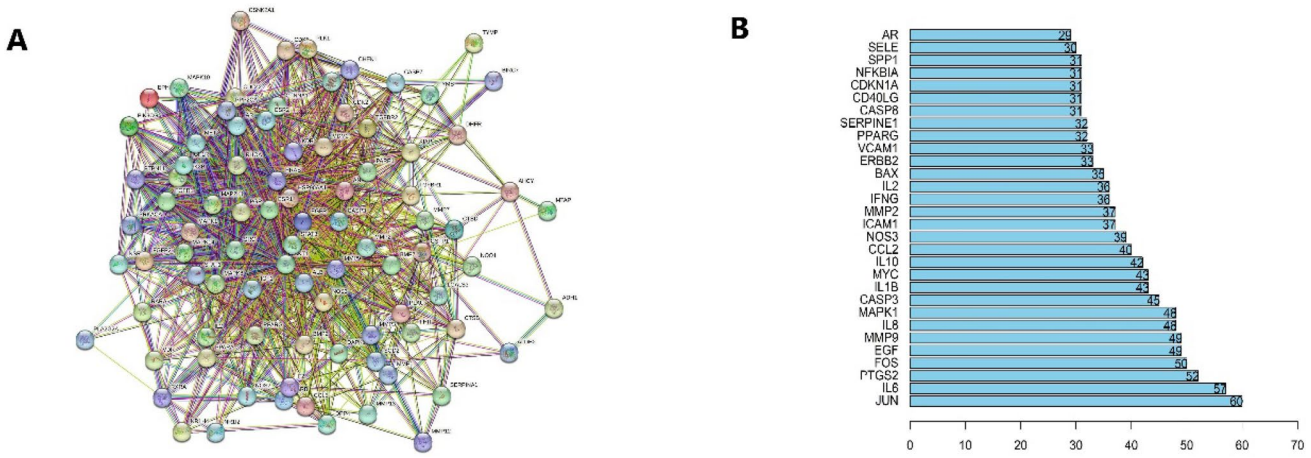

Fig. 4 PPI network and protein adjacency number bar graph. **A** Protein–protein interaction network. Blue represents interactions confirmed in the database, purple represents interactions confirmed in experiments, green represents interactions predicted in gene neighborhoods, red represents interactions predicted in gene fusions, dark blue represents interactions predicted in gene co-occurrence, yellow represents interactions predicted through text mining, black represents interactions predicted through co-expression, and light purple represents protein homology-based interaction predictions. **B** The bar graph of protein interactions. X-axis indicates the number of neighboring proteins of the target protein. Y-axis indicates the name of the target protein

3.5 Molecular docking

Molecular docking experiments were performed to investigate the interactions between PPI and key targets in HCC. Our results showed that PPI had good docking activity with the target proteins VEGF-C (PDB: 2X1X) and β-catenin (PDB: 3SL9). VEGF-C is a crucial regulator of HCC, while β-catenin is important for embryonic development, adult cell differentiation, and growth factors. Our molecular docking analysis revealed that PPI binds to VEGF-C by forming hydrogen bonds with LYSR: 286, ASPE: 139, GLYE: 145, and PHEE: 152, and forms hydrocarbon bonds with LYSR: 286, ASPR: 276, GLYE: 141, LYSE: 142, PROE: 155, and ASPE: 139 (Fig. 6A and B). Similarly, PPI binds to β-catenin by forming hydrocarbon bonds with ASNB: 204, THRB: 205, and ASPB: 162, and hydrogen bonds with GLNA: 203 (Fig. 6C and D). Notably, when docked, PPI forms LYS278 and ARG200 with VEGF-C and β-catenin, respectively, which may cause changes in the structure of the proteins. It may affect the function or expression of VEGF-C and β-catenin (Fig. 6B and D). In general, a lower energy binding conformational stability indicates a stronger interaction between the ligand and receptor pair. Our results showed that PPI has strong binding activity and reliable predictions when binding to both VEGF-C and β-catenin, with a binding activity of less than -6.0 kcal/mol. Detailed binding energy data are in Supplementary Table 8.

3.6 PPI inhibits tumor growth in a mouse orthotopic xenograft model

HCC can result in tumorous hepatomegaly, characterized by variations in size and shape compared to the normal liver, along with the presence of abnormal proliferative tumor tissue. To examine the therapeutic impact of PPI on HCC, we established a mouse orthotopic xenograft model. Two weeks after modeling, we observed that the liver volume of mice in the PP-treated group was smaller compared to the control group. Additionally, PPI intervention significantly reduced the white tumor foci on the surface of the mouse liver (Fig. 7A). It can be observed that the PPI treatment did not have a significant effect on the body weight of the tumor-bearing mice but significantly reduced the liver weight (Fig. 7B–D). After removing the tumor tissue, we also observed a significant decrease in tumor tissue weight in the PPI-treated group compared to the control group (Fig. 7E). The emitted photons from the tumors in mice were detected using the Xenogen IVIS imaging system. Treatment with PPI resulted in a decrease in the total photon flux in the liver (Fig. 7F and G). The results revealed that PPI can inhibit the growth of HCC in vivo.

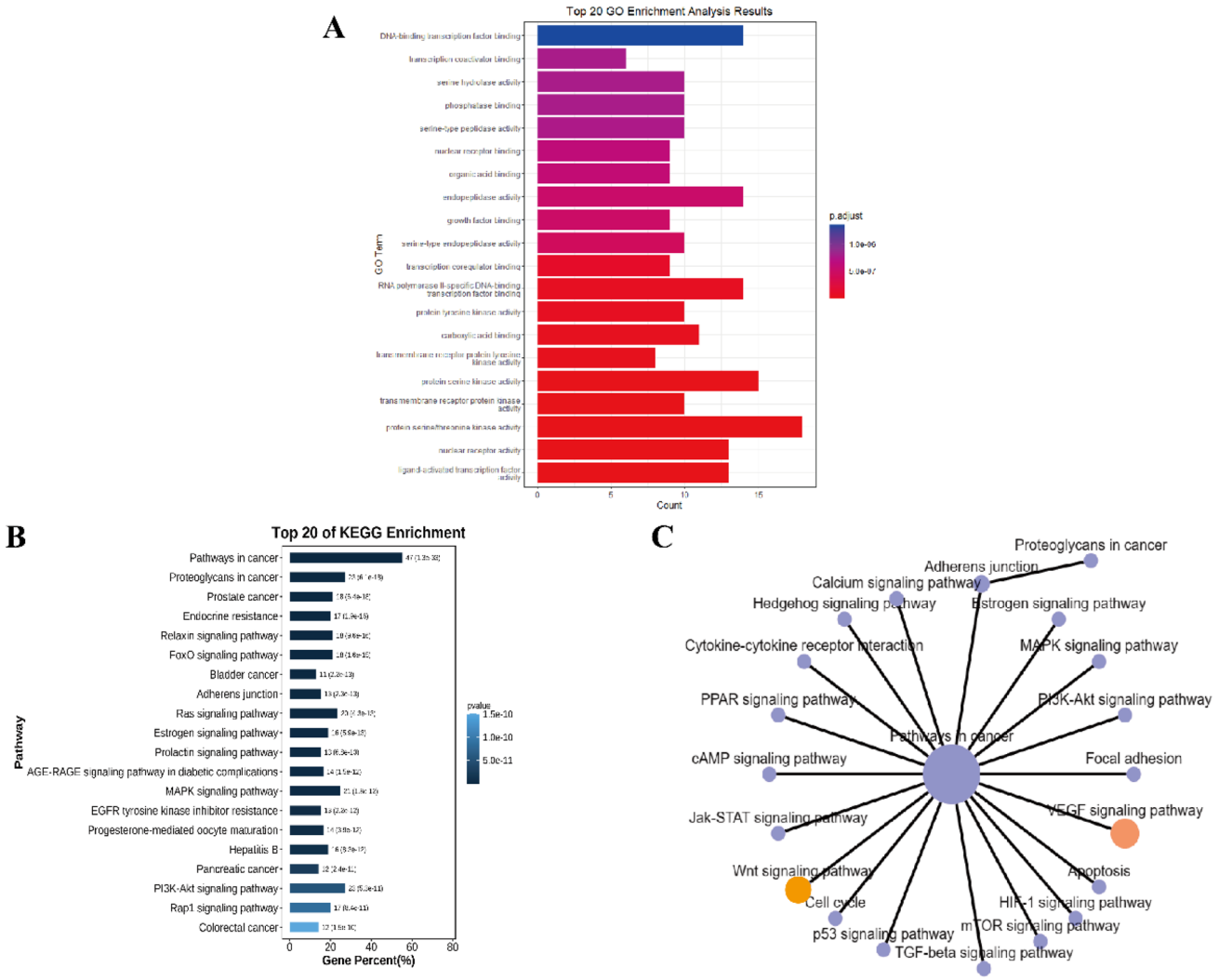

Fig. 5 Gene Ontology (GO) and Kyoto Encyclopedia of Genes and Genomes (KEGG) pathway analyses. **A** GO analysis was performed on 90 targets associated with HCC and PPI. X-axis indicates significant enrichment of measures for these terms. Y-axis shows the categories of biological processes in GO for targets ($p < 0.01$). **B** KEGG pathway enrichment analyses associated with HCC and PPI. The X-axis indicates the number of targets in each pathway. the Y-axis indicates the major pathways. **C** All signaling pathways included in the cancer pathway associated with HCC and PPI

3.7 PPI inhibits cell proliferation and promotes apoptosis of MHCC-97H cells

To evaluate the effects of PPI on HCC cell proliferation and apoptosis, we conducted CCK8 and flow cytometry assays on MHCC-97H cells. As shown in Fig. 8A and B, PPI significantly inhibited the survival of MHCC-97H cells in a dose-dependent manner, with an IC50 value of 2.327 μM. As illustrated in Fig. 8C and D, 1 μM PPI treatment for 24 h had no effect on cell apoptosis, whereas the treatment with 2.5 μM PPI for 24 h significantly induced apoptosis in MHCC-97H cells. These results confirm the ability of PPI to inhibit HCC proliferation and promote apoptosis.

3.8 PPI inhibits MHCC-97H cell metastasis

To investigate the effects of PPI on the invasion and migration abilities of human HCC cells, we performed transwell invasion and wound healing assays. The results of the transwell invasion assay showed that PPI treatment at 1 μM and 2.5 μM for 24 h significantly inhibited the invasion of MHCC-97H cells (Fig. 9A and B). Additionally, the results of

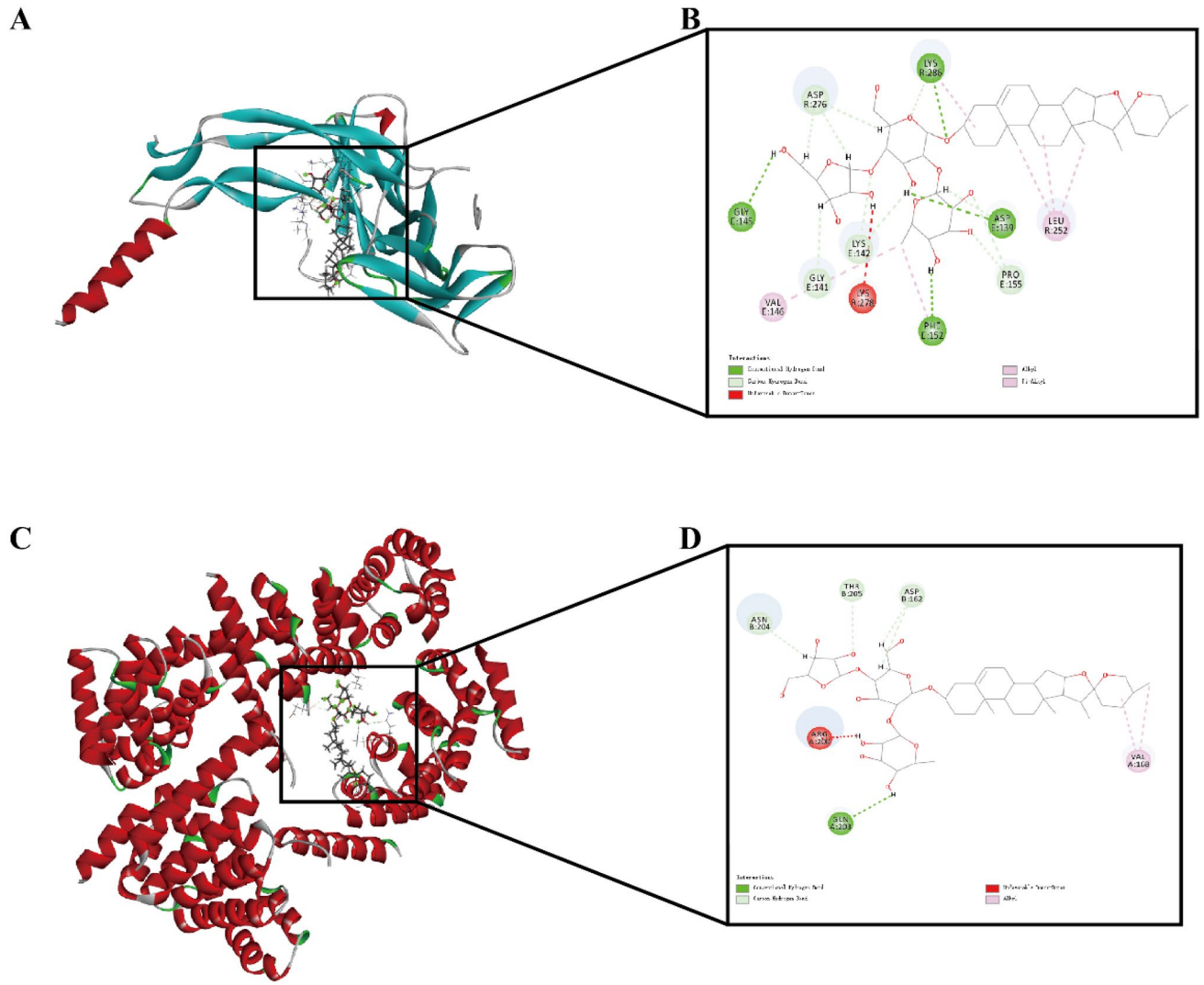

Fig. 6 The molecular docking models of interactions between PPI and its predicted protein targets. **A** PPI and VEGF-C (PBD: 2X1X). **B** 2D binding site diagram of PPI and VEGF-C. **C** PPI and β-catenin (PDB: 3SL9). **D** 2D binding site diagram of PPI and β-catenin

the wound healing assay demonstrated that the percentage of wound closure in the groups treated with 1 μM and 2.5 μM PPI for 24 h and 48 h was significantly reduced compared to the control group (Fig. 9C and D). These results confirm the ability of PPI to inhibit the cell metastasis of HCC cells.

3.9 PPI inhibits the mRNA and protein levels of VEGF-C and β-catenin in MHCC-97H cells

We assessed VEGF-C and β-catenin mRNA and protein expression in MHCC-97H cells following PPI treatment using RT-qPCR and Western blot. After 24 h of treatment, VEGF-C and β-catenin mRNA levels in MHCC-97H cells significantly decreased (Fig. 10A and B). Similarly, a marked reduction in VEGF-C and β-catenin protein levels was observed in MHCC-97H cells of the PPI group after 24 h of treatment compared to the control group (Fig. 10C-E). These findings indicate that PPI may exert its therapeutic effects on HCC by inhibiting the VEGF-C and Wnt/β-catenin signaling pathways.

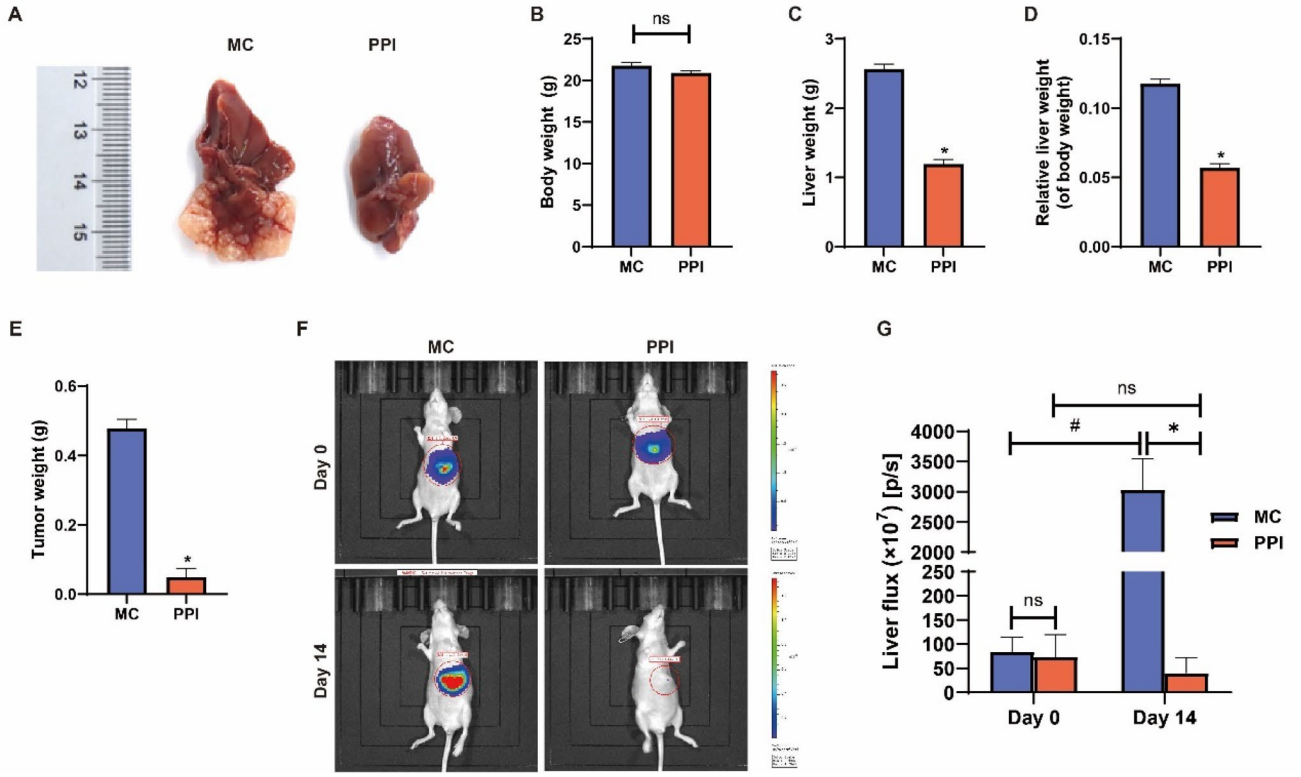

Fig. 7 PPI suppressed the tumor growth in MHCC-97H luciferase cell-xenografted animals. **A** Liver tissue. **B** Body weight. **C** Liver weight. **D** Relative liver weight. **E** Tumor weight. **F** Representative images of luciferase expression obtained immediately before the treatment (Day 0) and after treatment of PPI for 2 weeks (Day 14). **G** Quantification results of luciferase signal intensity of tumors in liver. The data are shown as the means ± SEM ($n = 5$). PPI: 10 mg/kg/d PPI intervention group, n = 5; MC: the model control group. $^{*}P < 0.05$ PPI vs. MC; $^{\#}P < 0.05$ Day 14 vs. Day 0

4 Discussion

Natural medicines have attracted widespread attention due to their complex active ingredients and wide range of pharmacological effects. The anti-cancer mechanism of active ingredients in natural medicines has attracted particular attention. As a promising natural medicine with anti-cancer properties, *Paris polyphylla* (Chinese name: Chonglou) has shown significant therapeutic potential. PPI, a key active ingredient of *Paris polyphylla*, exhibits strong antitumor activities in various cancers, including HCC [15, 38–41]. Its anti-tumor effects are primarily manifested in inducing cell apoptosis [42], promoting cancer cell ferroptosis [15, 39], autophagy [16, 42], and cell cycle arrest [43, 44], as well as inhibiting cell migration and invasion [45]. Consistent with previous studies, our findings demonstrated that PPI effectively suppressed the growth of xenograft tumors in mice and inhibited the viability of MHCC-97H cells, highlighting its promising potential for HCC treatment.

Identifying drug targets and disease-related targets is crucial for drug discovery and development, as both drugs and diseases involve the regulation of multiple targets [46–48]. In this study, we predicted 293 potential therapeutic targets of PPI using SwissTargetPrediction, PharmMapper, and STITCH databases. Additionally, we identified 1206 HCC-related targets using the GeneCards, OMIM, and PharmGKB databases. The intersection of these two datasets yielded 90 overlapping genes, representing potential targets of PPI in HCC treatment. Protein–protein interaction network is essential for cellular activities and biological functions across all living organisms. Therefore, the protein–protein interaction network is a valuable tool for investigating the complexities of cellular processes and signaling pathways [49]. We constructed a protein–protein interaction network using the 90 overlapping targets and analyzed the network topology to identify key targets based on their connectivity. Our analysis revealed that 30 targets, including JUN, IL6, PTGS2, FOS, EGF, MMP9, IL8, MAPK1, and CASP3, exhibited high connectivity, suggesting their crucial roles in PPI's anti-HCC effects. These targets are all associated with critical cellular processes involved in

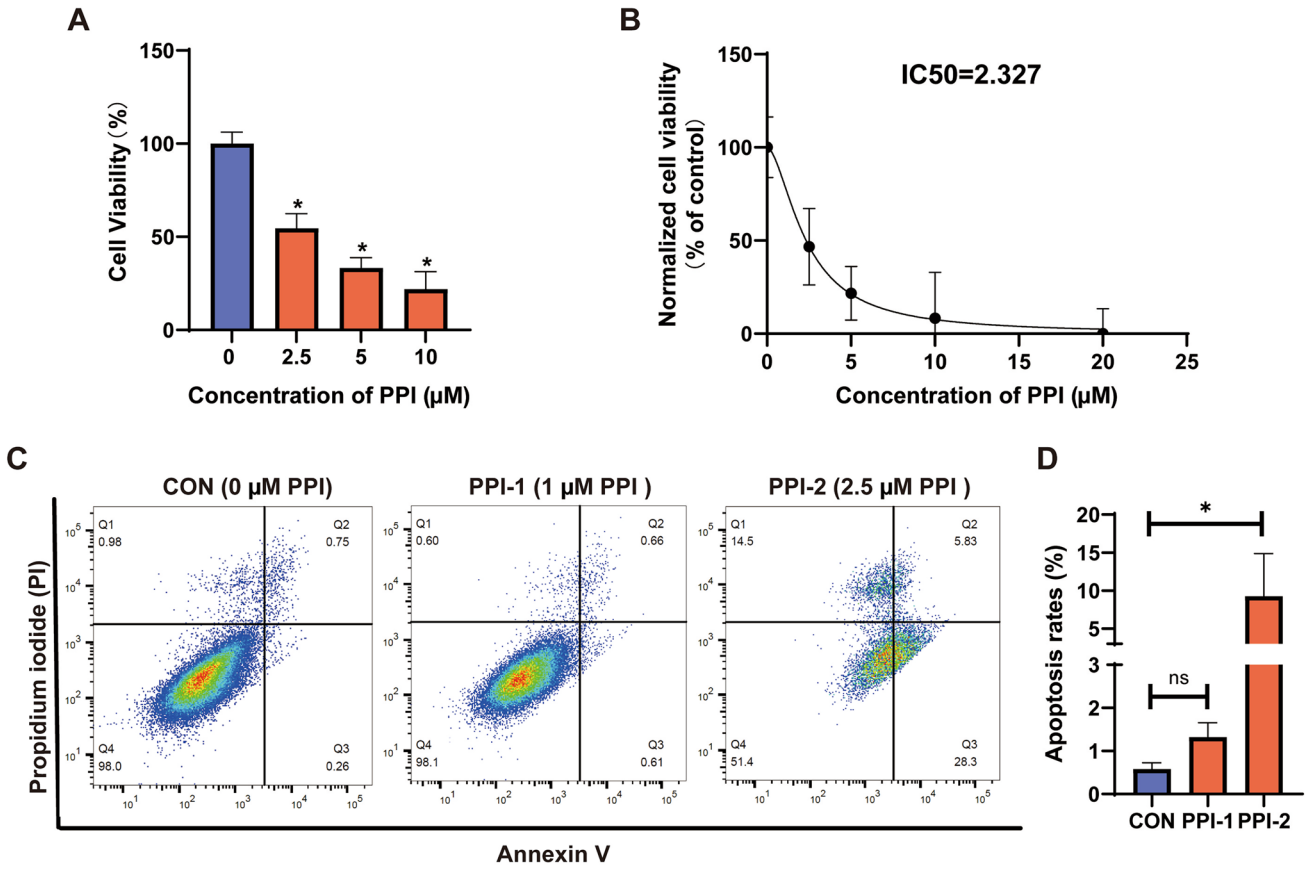

Fig. 8 PPI inhibited MHCC-97H cells proliferation and induced cellular apoptosis. **A** The cell viability detected by CCK8 assay. **B** Cell survival curve with the IC50 values. **C** Apoptosis analysis by flow cytometry after Annexin V-FITC/ PI staining. **D** The apoptosis rates. The data are shown as the means ± SEM ($n = 3$). CON: control group (0 μM PPI), PPI-1: 1 μM PPI treatment group, PPI-2: 2.5 μM PPI treatment group. *$P < 0.05$ PPI vs. CON

HCC development and progression, such as cell proliferation, apoptosis, and migration, supporting the notion that PPI may exert its therapeutic effects through a multi-target mechanism.

GO and KEGG enrichment analyses of the 90 overlapping targets revealed that PPI targets are significantly enriched in pathways related to cell proliferation, cell cycle regulation, cell migration and invasion, and apoptosis. This suggested that PPI might exert its anti-HCC effects by modulating these key cellular processes. Further analysis of the "Pathways in cancer" category, which ranked first in the KEGG pathway enrichment analysis, highlighted the involvement of the VEGF and Wnt/β-catenin signaling pathways. VEGF-C and Wnt/β-catenin signaling pathways play crucial roles in HCC development and progression, affecting various hallmarks of cancer, including angiogenesis, cell proliferation, survival, and metastasis [50, 51]. These findings suggested that the regulation of proliferation, apoptosis, migration, and invasion might be one of the primary factors contributing to the therapeutic effects of PPI in HCC treatment. These results provided valuable insights for our subsequent experimental validation focus and guided us to investigate the impact of PPI on the VEGF-C and Wnt/β-catenin signaling pathways.

The binding site of a drug to its therapeutic target plays a crucial role in the stability of the drug-target complex [46–48]. Therefore, identifying the binding site is generally considered essential for drug discovery and development. Based on the KEGG analysis, we found that the VEGF and Wnt/β-catenin signaling pathways play critical roles in HCC, prompting us to analyze the binding sites and binding potential of PPI with targets in these pathways using molecular docking. Our results showed that PPI exhibited binding energies of less than -6 kcal/mol with VEGF-C and β-catenin, indicating a high binding affinity. The binding force of VEGF-C and β-catenin for PPI primarily originated from hydrogen bonds, which contribute to the stability of their binding modes. Further analysis of the binding mode of PPI to VEGF-C and β-catenin revealed that PPI can also produce residues Lys:278 (VEGF-C) and Arg:200 (β-catenin) with them, which may induce protein structural rearrangement of VEGF-C and β-catenin. Specifically, the positively charged side chains of Lys278 (VEGF-C) and Arg200 (β-catenin) can distort the local structural motifs through salt

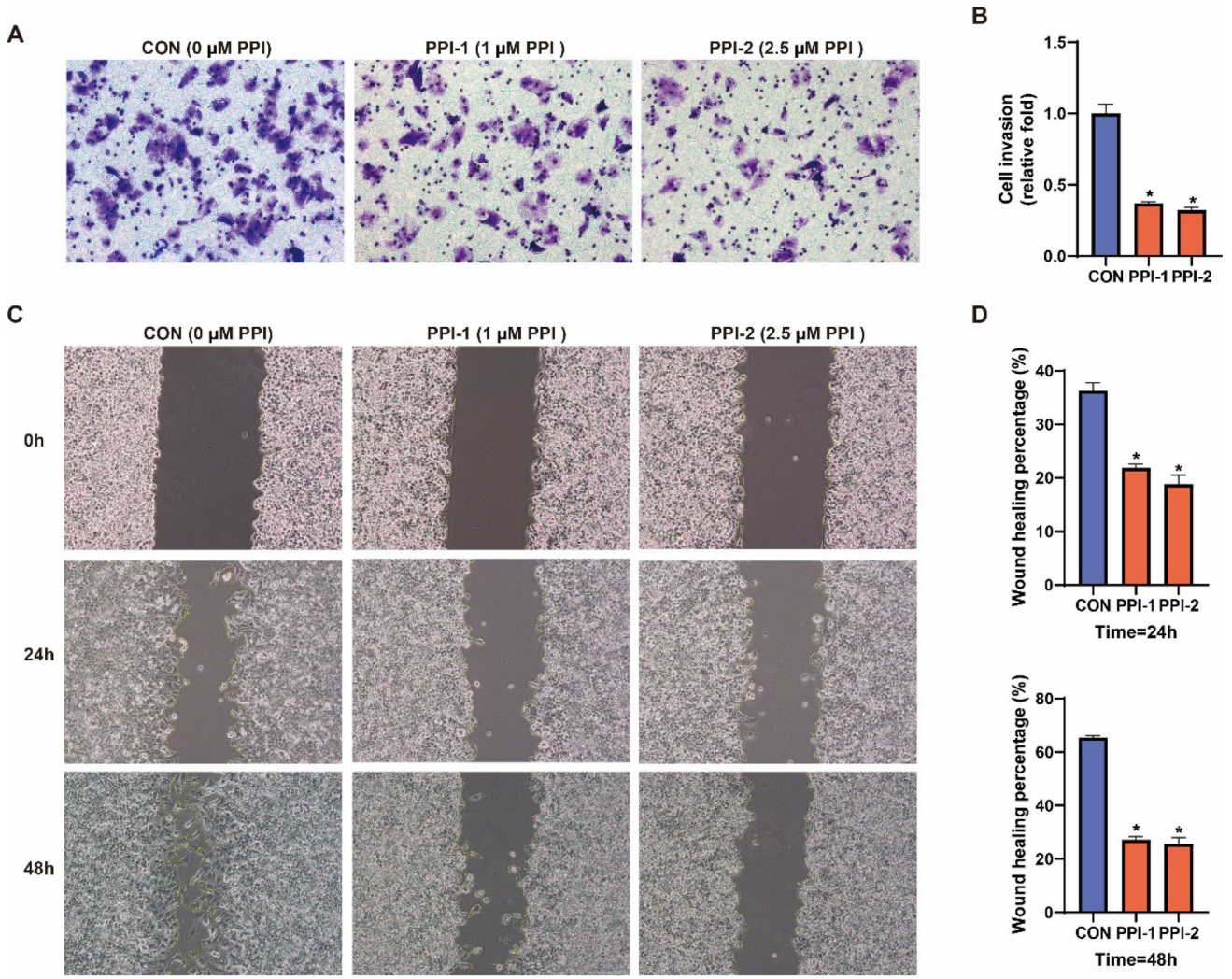

Fig. 9 PPI inhibited MHCC-97H cells migration and invasion. **A** Transwell invasion of MHCC-97H cells. **B** Quantification results of cell invasion of MHCC-97H cells. **C** Wound healing scratch assay of MHCC-97H cells. **D** Quantification results of the wound healing percentage of MHCC-97H cells. The data are shown as the means ± SEM ($n = 3$). CON: control group (0 μM PPI), PPI-1: 1 μM PPI treatment group, PPI-2: 2.5 μM PPI treatment group. *$P < 0.05$ PPI-1/2 vs. CON

bridges or hydrogen bonds. This interference may change the signal transduction ability mediated by VEGF-C or β-catenin, thereby inhibiting the VEGF-C and Wnt/β-catenin signaling pathways.

The results in vivo demonstrated that PPI treatment significantly reduced tumor weight, volume, and photon flux in a mouse orthotopic xenograft model. This finding was consistent with previous studies using subcutaneous HCC xenograft models, who demonstrated that PPI suppresses HCC progression through ferroptosis induction [15]. However, our study utilized an orthotopic xenograft model, which more closely mimics the tumor microenvironment and metastatic potential of HCC in humans compared to subcutaneous models. This approach provided a more accurate assessment of PPI's therapeutic efficacy in a clinically relevant setting. In vitro studies using MHCC-97H cells confirmed anti-HCC effects of PPI, demonstrating significant inhibition of cell proliferation, migration, and invasion, as well as induction of apoptosis. These observations aligned with previous in vitro studies using various HCC cell lines, including HepG2, SMMC-7721, and Huh7, which have reported similar inhibitory effects of PPI on cell proliferation, migration, and invasion [13, 16, 45]. Additionally, we observed a significant downregulation of VEGF-C and β-catenin expression at both mRNA and protein levels in PPI-treated HCC cells, supporting the involvement of these pathways in the anti-HCC effects of PPI. This also further validated our result of network pharmacology pathway prediction and provided strong evidence for the potential of PPI in HCC treatment.

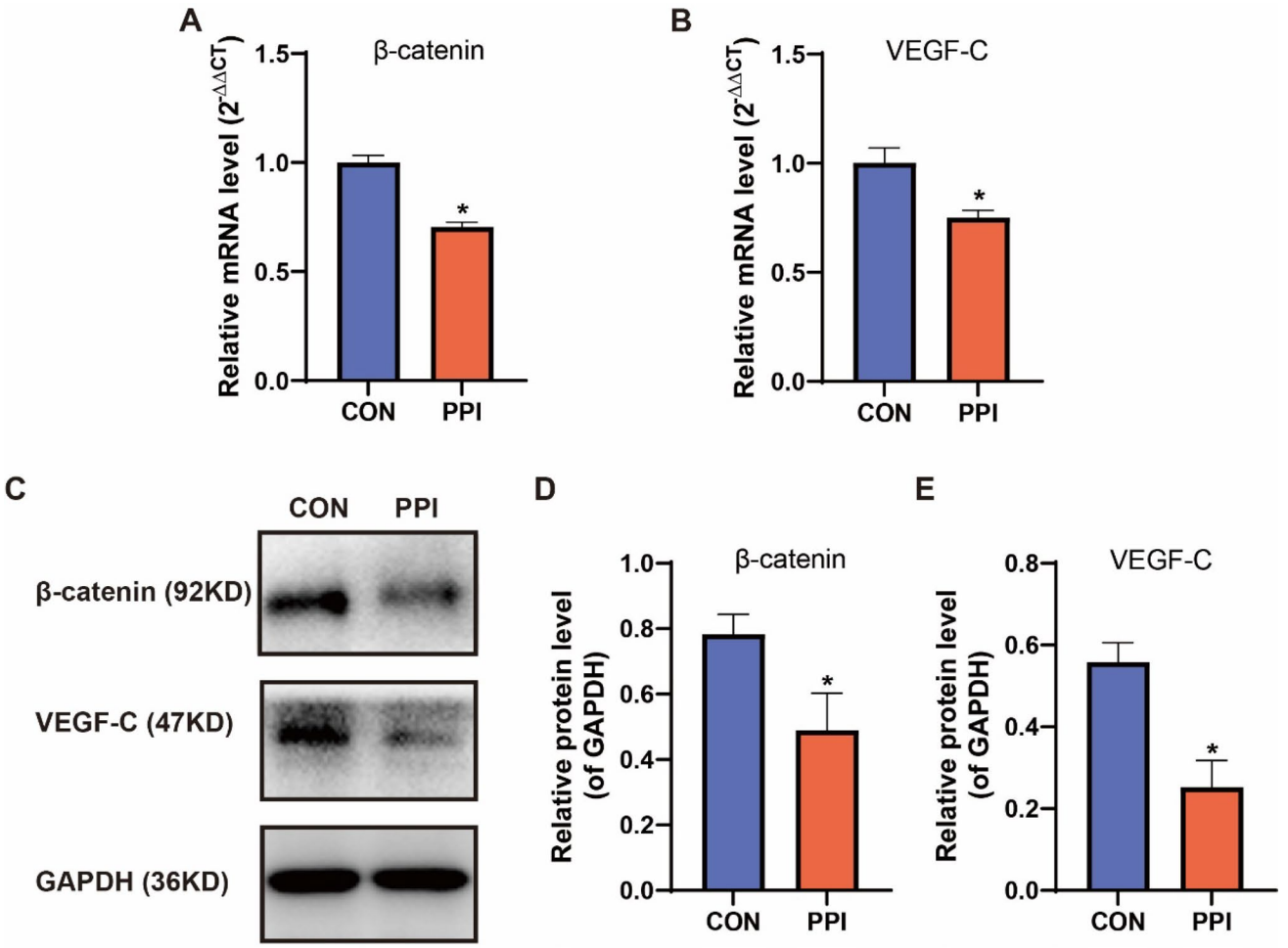

Fig. 10 PPI inhibited mRNA and protein expression of β-catenin and VEGF-C in MHCC-97H cells. **A** Relative expression of β-catenin mRNA and (**B**) VEGF-C mRNA detected by RT-qPCR assay. **C** β-catenin and VEGF-C protein levels detected by western blot assay. **D** Quantitative relative expression of β-catenin protein and (**E**) VEGF-C protein. Relative mRNA and protein expression were normalized by GAPDH. The data are shown as the means ± SEM ($n \geq 3$). CON: control group (0 μM PPI), PPI: 2.5 μM PPI treatment group. *$P < 0.05$ PPI vs. CON

VEGF-C, a member of the VEGF family, is a potent driver of lymphangiogenesis, contributing to tumor cell dissemination and metastasis [52, 53]. Elevated VEGF-C expression in HCC is associated with advanced tumor stage, lymph node metastasis, and poor prognosis [54]. Previous studies have shown that PPI can inhibit HCC cell proliferation and metastasis by inducing ferroptosis through the Nrf2/HO-1/GPX4 axis [15] or targeting the ZBTB16/PPARγ/RXRα axis in HCC cells [14]. PPI can also exert anti-sorafenib-resistant HCC activity both in vitro and in vivo by modulating GRP78 activity [45]. Although previous reports have demonstrated that PPI has therapeutic effects on HCC primarily by targeting VEGF-A [55], the impact of PPI on VEGF-C (a key driver of lymphangiogenesis) remain underexplored. Unlike previous studies, our findings highlighted that PPI may exert antitumor activity in HCC by targeting VEGF-C. Moreover, our molecular docking and KEGG pathway analysis results suggested that PPI might directly inhibit VEGF-C signaling by binding to VEGFR2, thereby reducing HCC metastasis and proliferation (Fig. 11). There have been reports of other compounds, such as oxyresveratrol and resveratrol, targeting VEGF-C/VEGFR3 to inhibit HCC angiogenesis and lymphatic metastasis [56]. Compared to these, the concentrations of PPI used in our study (2.5 μM in vitro, 10 mg/kg in vivo) were lower. In addition to inhibiting tumor growth and metastasis, we also found that PPI can promote apoptosis, demonstrating a broader range of effects.

The Wnt/β-catenin pathway, composed of Wnt proteins, Wnt protein ligands and regulatory proteins, maintains cell homeostasis by regulating cell proliferation, differentiation, movement and apoptosis [57]. Previous studies have demonstrated that PPI can inhibit HCC cell proliferation and promote apoptosis by acting on the AKT/GSK-3β/β-catenin signaling pathway [13]. Consistent with these findings, our network pharmacology and molecular docking analyses suggested that PPI may target Wnt/β-catenin pathway-related targets, such as GSK3B, AKT1 and MAPK1, to exert its

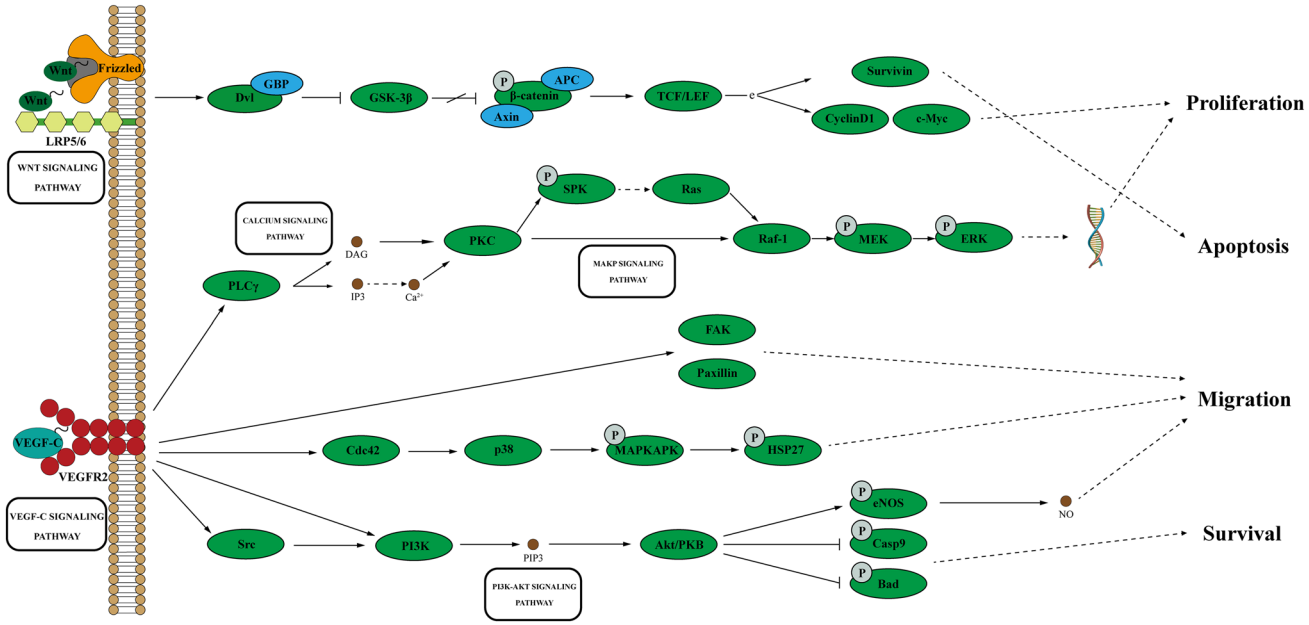

Fig. 11 KEGG-derived VEGF and Wnt/β-catenin signaling pathway maps

therapeutic effects in HCC (Fig. 11). In contrast to other reported compounds that may target β-catenin-related pathways to exert anti-HCC activity, our study differed significantly in experimental models and design. It has been reported that Bruceine D inhibits the Jagged1 transcription by suppressing the Wnt/β-catenin pathway in a dose-dependent manner, thereby significantly inhibiting HCC growth, and enhancing the therapeutic effects of sorafenib [58]. Similarly, Aucubin has been found to exert anti-HCC activity by inhibiting the Akt/β-catenin/PD-L1 axis, and it also enhances the antitumor effects of cisplatin [59]. In comparison, we used a different high-metastatic MHCC-97H HCC cell line and its corresponding orthotopic xenograft model in our experiments. Additionally, our study did not investigate the impact of PPI on the efficacy of currently used clinical treatments for HCC.

This study provided strong evidence for the therapeutic potential of PPI in HCC treatment and elucidated its possible mechanisms, including the modulation of the VEGF-C and Wnt/β-catenin signaling pathways. Despite our promising findings, several limitations must be considered. Firstly, we did not elucidate the upstream and downstream molecular mechanisms through which PPI regulates the VEGF-C and Wnt/β-catenin pathways. Secondly, our study did not include experiments with different concentrations of PPI, so we were unable to investigate the dose-dependent effects of PPI on the VEGF-C and Wnt/β-catenin pathways. Furthermore, the relatively short duration of the animal study precluded survival analysis in tumor-bearing mice. Finally, although our experiments demonstrated the efficacy of PPI in MHCC-97H cells and animal models, and other studies have also reported similar effects in different HCC cell lines [17, 45], the heterogeneity between different cell types and species means that our findings are limited to a single cell model and cannot be generalized to other HCC cell lines. Therefore, future studies should include specific mechanistic investigations of the upstream and downstream targets, dose-dependent analysis with a range of PPI concentrations, observations over longer research periods and experimental validation in a broader set of HCC cell lines and more complex animal models to more comprehensively assess the therapeutic potential of PPI.

5 Conclusion

In summary, this study explored the potential mechanism of PPI inhibition of HCC by integrating network pharmacology, molecular docking and in vitro and in vivo experimental verification. The results suggest that PPI may induce cell apoptosis, inhibit the cell proliferation, migration and invasion of the MHCC-97H cells through suppressing the Wnt/β-catenin and VEGF-C signaling pathways.

Acknowledgements Not applicable.

Author contributions Jiamei Le contributed to the design of the study. Yilong Chen conducted network pharmacologic analysis, prepared diagrams and wrote the manuscript. Qiuying Wang, Shuixiu Bian, and Jing Dong performed the verification experiments and processed the data. Jiamei Le and Jie Xiong revised the manuscript.

Funding This work was supported by grants from National Natural Science Foundation of China (81903961), Shanghai Key Laboratory of Molecular Imaging (18DZ2260400), Shanghai Science and Technology Innovation Action Plan (Laboratory Animal Research Project, 22140902200), Climbing Program of Shanghai University of Medicine & Health Sciences (A3-2601–24-311001).

Data availability All data supporting the findings of this study are available within the paper and its Supplementary Information.

Code availability Not applicable.

Declarations

Ethics approval and consent to participate The animal study was approved by The Institutional Animal Care and Use Committee (IACUC) of Shanghai University of Medicine & Health Sciences, with the permit number: 2023SY052. All animal experimental procedures were conducted in accordance with the local legislation and institutional requirements. The maximal tumor burden permitted by the ethics committee is 10% of the animal's body weight. We confirm that no tumors exceeded the approved limit of 10% of the animal's body weight throughout the duration of the study. In cases where it has been exceeded, humane endpoints were implemented as per the ethical guidelines to ensure animal welfare.

Consent for publication Not applicable.

Competing interests The authors declare no competing interests.

References

1. Rumgay H, Arnold M, Ferlay J, Lesi O, Cabasag CJ, Vignat J, Laversanne M, McGlynn KA, Soerjomataram I. Global burden of primary liver cancer in 2020 and predictions to 2040. J Hepatol. 2022;77:1598–606.
2. Sung H, Ferlay J, Siegel RL, Laversanne M, Soerjomataram I, Jemal A, Bray F. Global cancer statistics 2020: GLOBOCAN estimates of incidence and mortality worldwide for 36 cancers in 185 countries. Cancer J Clin. 2021. https://doi.org/10.1016/S0140-6736(22)01200-4.
3. Vogel A, Meyer T, Sapisochin G, Salem R, Saborowski A. Hepatocellular carcinoma. Lancet. 2022;400:1345–62.
4. Yang JD, Hainaut P, Gores GJ, Amadou A, Plymoth A, Roberts LR. A global view of hepatocellular carcinoma: trends, risk, prevention and management. Nat Rev Gastroenterol Hepatol. 2019;16:589–604.
5. Rinaldi L, Vetrano E, Rinaldi B, Galiero R, Caturano A, Salvatore T, Sasso FC. HCC and molecular targeting therapies: back to the future. Biomedicines. 2021;9:1345.
6. Llovet JM, Pinyol R, Kelley RK, El-Khoueiry A, Reeves HL, Wang XW, Gores GJ, Villanueva A. Molecular pathogenesis and systemic therapies for hepatocellular carcinoma. Nature cancer. 2022;3:386–401.
7. Kudo M, Finn RS, Qin S, Han KH, Ikeda K, Piscaglia F, Baron A, Park JW, Han G, Jassem J, Blanc JF, Vogel A, Komov D, Evans TRJ, Lopez C, Dutcus C, Guo M, Saito K, Kraljevic S, Tamai T, Ren M, Cheng AL. Lenvatinib versus sorafenib in first-line treatment of patients with unresectable hepatocellular carcinoma: a randomised phase 3 non-inferiority trial. Lancet. 2018;391:1163–73.
8. Tang W, Chen Z, Zhang W, Cheng Y, Zhang B, Wu F, Wang Q, Wang S, Rong D, Reiter FP, De Toni EN, Wang X. The mechanisms of sorafenib resistance in hepatocellular carcinoma: theoretical basis and therapeutic aspects. Signal Transduct Target Ther. 2020;5:87.
9. Matos LC, Machado JP, Monteiro FJ, Greten HJ. Understanding traditional Chinese medicine therapeutics: an overview of the basics and clinical applications. Healthcare. 2021;9:257.
10. Xu H, Zhao X, Liu X, Xu P, Zhang K, Lin X. Antitumor effects of traditional Chinese medicine targeting the cellular apoptotic pathway. Drug Des Devel Ther. 2015;9:2735–44.
11. Tian Y, Gong G-Y, Ma L-L, Wang Z-Q, Song D, Fang M-Y. Anti-cancer effects of Polyphyllin I: an update in 5 years. Chem Biol Interact. 2020;316:108936.
12. Li J, Jia J, Zhu W, Chen J, Zheng Q, Li D. Therapeutic effects on cancer of the active ingredients in rhizoma paridis. Front Pharmacol. 2023;14:1095786.
13. Liao M, Du H, Wang B, Huang J, Huang D, Tong G. Anticancer effect of Polyphyllin I in suppressing stem cell-like properties of hepatocellular carcinoma via the AKT/GSK-3β/β-catenin signaling pathway. Oxid Med Cell Longev. 2022;2022:4031008.
14. Shan L, Chen Y, An G, Tao X, Qiao C, Chen M, Li J, Lin R, Wu J, Zhao C. Polyphyllin I exerts anti-hepatocellular carcinoma activity by targeting ZBTB16 to activate the PPARγ/RXRα signaling pathway. Chin Med. 2024;19:113.

15. Yang R, Gao W, Wang Z, Jian H, Peng L, Yu X, Xue P, Peng W, Li K, Zeng P. Polyphyllin I induced ferroptosis to suppress the progression of hepatocellular carcinoma through activation of the mitochondrial dysfunction via Nrf2/HO-1/GPX4 axis. Phytomedicine. 2024;122: 155135.
16. Shi YM, Yang L, Geng YD, Zhang C, Kong LY. Polyphyllin I induced-apoptosis is enhanced by inhibition of autophagy in human hepatocellular carcinoma cells. Phytomedicine. 2015;22:1139–49.
17. Xiao T, Zhong W, Zhao J, Qian B, Liu H, Chen S, Qiao K, Lei Y, Zong S, Wang H, Liang Y, Zhang H, Meng J, Zhou H, Sun T, Liu Y, Yang C. Polyphyllin I suppresses the formation of vasculogenic mimicry via Twist1/VE-cadherin pathway. Cell Death Dis. 2018;9:906.
18. Hao DC, Xiao PG. Network pharmacology: a Rosetta Stone for traditional Chinese medicine. Drug Dev Res. 2014;75:299–312.
19. Wu W, Zhang Z, Li F, Deng Y, Lei M, Long H, Hou J, Wu W. A Network-based approach to explore the mechanisms of uncaria alkaloids in treating hypertension and alleviating Alzheimer's disease. Int J Mol Sci. 2020. https://doi.org/10.3390/ijms21051766.
20. Poornima P, Kumar JD, Zhao Q, Blunder M, Efferth T. Network pharmacology of cancer: from understanding of complex interactomes to the design of multi-target specific therapeutics from nature. Pharmacol Res. 2016;111:290–302.
21. Hopkins AL. Network pharmacology: the next paradigm in drug discovery. Nat Chem Biol. 2008;4:682–90.
22. Gfeller D, Grosdidier A, Wirth M, Daina A, Michielin O, Zoete V. SwissTargetPrediction: a web server for target prediction of bioactive small molecules. Nucleic Acids Res. 2014;42:W32–8.
23. Liu X, Ouyang S, Yu B, Liu Y, Huang K, Gong J, Zheng S, Li Z, Li H, Jiang H. PharmMapper server: a web server for potential drug target identification using pharmacophore mapping approach. Nucleic Acids Res. 2010;38:W609–14.
24. Wang X, Pan C, Gong J, Liu X, Li H. Enhancing the enrichment of pharmacophore-based target prediction for the polypharmacological profiles of drugs. J Chem Inf Model. 2016;56:1175–83.
25. Wang X, Shen Y, Wang S, Li S, Zhang W, Liu X, Lai L, Pei J, Li H, PharmMapper,. update: a web server for potential drug target identification with a comprehensive target pharmacophore database. Nucleic Acids Res. 2017;45(2017):W356–60.
26. Stelzer G, Rosen N, Plaschkes I, Zimmerman S, Twik M, Fishilevich S, Stein TI, Nudel R, Lieder I, Mazor Y, Kaplan S, Dahary D, Warshawsky D, Guan-Golan Y, Kohn A, Rappaport N, Safran M, Lancet D. The genecards suite: from gene data mining to disease genome sequence analyses. Curr Protoc Bioinform. 2016;54:1.
27. Amberger JS, Hamosh A. Searching online Mendelian inheritance in Man (OMIM): a knowledgebase of human genes and genetic phenotypes. Curr Protoc Bioinform. 2017;58:1.
28. Whirl-Carrillo M, McDonagh EM, Hebert JM, Gong L, Sangkuhl K, Thorn CF, Altman RB, Klein TE. Pharmacogenomics knowledge for personalized medicine. Clin Pharmacol Ther. 2012;92:414–7.
29. Coudert E, Gehant S, de Castro E, Pozzato M, Baratin D, Neto T, Sigrist CJA, Redaschi N, Bridge A. Annotation of biologically relevant ligands in UniProtKB using ChEBI. Bioinformatics. 2023;39:btac793.
30. Shannon P, Markiel A, Ozier O, Baliga NS, Wang JT, Ramage D, Amin N, Schwikowski B, Ideker T. Cytoscape: a software environment for integrated models of biomolecular interaction networks. Genome Res. 2003;13:2498–504.
31. Szklarczyk D, Kirsch R, Koutrouli M, Nastou K, Mehryary F, Hachilif R, Gable AL, Fang T, Doncheva NT, Pyysalo S, Bork P, Jensen LJ, von Mering C, The STRING, database in,. protein-protein association networks and functional enrichment analyses for any sequenced genome of interest. Nucleic Acids Res. 2023;51(2023):D638–46.
32. Yu G, Wang L-G, Han Y, He Q-Y. clusterProfiler: an R package for comparing biological themes among gene clusters. OMICS. 2012;16:284–7.
33. He J, Yu S, Guo C, Tan L, Song X, Wang M, Wu J, Long Y, Gong D, Zhang R, Cao Z, Li Y, Peng C. Polyphyllin I induces autophagy and cell cycle arrest via inhibiting PDK1/Akt/mTOR signal and downregulating cyclin B1 in human gastric carcinoma HGC-27 cells. Biomed Pharmacother Biomed Pharmacother. 2019;117:109189.
34. Zhang X, Lu X, Shi J, Li Y, Li Y, Tao R, Huang L, Tang Y, Zhu X, Li M, Gao Y, Feng H, Yu Z. Bufalin suppresses hepatocellular carcinogenesis by targeting M2 macrophage-governed Wnt1/β-catenin signaling. Phytomedicine. 2024;126: 155395.
35. Hu J, Shi Q, Xue C, Wang Q. Berberine protects against hepatocellular carcinoma progression by regulating intrahepatic T cell heterogeneity. Adv Sci. 2024;11: e2405182.
36. Goel HL, Mercurio AM. VEGF targets the tumour cell. Nat Rev Cancer. 2013;13:871–82.
37. Yu F, Yu C, Li F, Zuo Y, Wang Y, Yao L, Wu C, Wang C, Ye L. Wnt/β-catenin signaling in cancers and targeted therapies. Signal Transduct Target Ther. 2021;6:307.
38. Shen Z, Wang J, Ke K, Chen R, Zuo A, Zhang R, Wan W, Xie X, Li X, Song N, Fu H, Zhang Z, Cai E, Shen J, Zhang Q, Shi X. Polyphyllin I, a lethal partner of Palbociclib, suppresses non-small cell lung cancer through activation of p21/CDK2/Rb pathway in vitro and in vivo. Cell Cycle. 2021;20:2494–506.
39. Zheng F, Wang Y, Zhang Q, Chen Q, Liang CL, Liu H, Qiu F, Chen Y, Huang H, Lu W, Dai Z. Polyphyllin I suppresses the gastric cancer growth by promoting cancer cell ferroptosis. Front Pharmacol. 2023;14:1145407.
40. Xiang S, Zou P, Wu J, Zheng F, Tang Q, Zhou J, Hann SS. Crosstalk of NF-κB/P65 and LncRNA HOTAIR-mediated repression of MUC1 expression contribute to synergistic inhibition of castration-resistant prostate cancer by polyphyllin 1–enzalutamide combination treatment. Cell Physiol Biochem. 2018;47:759–73.
41. Li GB, Fu RQ, Shen HM, Zhou J, Hu XY, Liu YX, Li YN, Zhang HW, Liu X, Zhang YH, Huang C, Zhang R, Gao N. Polyphyllin I induces mitophagic and apoptotic cell death in human breast cancer cells by increasing mitochondrial PINK1 levels. Oncotarget. 2017;8:10359–74.
42. Luo Q, Jia L, Huang C, Qi Q, Jahangir A, Xia Y, Liu W, Shi R, Tang L, Chen Z. Polyphyllin I promotes autophagic cell death and apoptosis of colon cancer cells via the ROS-inhibited AKT/mTOR pathway. Int J Mol Sci. 2022. https://doi.org/10.3390/ijms23169368.
43. Li HS, Xu Y. Inhibition of EZH2 via the STAT3/HOTAIR signalling axis contributes to cell cycle arrest and apoptosis induced by polyphyllin I in human non-small cell lung cancer cells. Steroids. 2020;164: 108729.
44. Hong M, Almutairi MM, Li S, Li J. Wogonin inhibits cell cycle progression by activating the glycogen synthase kinase-3 beta in hepatocellular carcinoma. Phytomedicine. 2020;68: 153174.
45. Du H, Wu H, Kang Q, Liao M, Qin M, Chen N, Huang H, Huang D, Wang P, Tong G. Polyphyllin I attenuates the invasion and metastasis via downregulating GRP78 in drug-resistant hepatocellular carcinoma cells. Aging. 2023;15:12251–63.

46. Li YH, Yu CY, Li XX, Zhang P, Tang J, Yang Q, Fu T, Zhang X, Cui X, Tu G, Zhang Y, Li S, Yang F, Sun Q, Qin C, Zeng X, Chen Z, Chen YZ, Zhu F, Therapeutic target database update,. enriched resource for facilitating bench-to-clinic research of targeted therapeutics. Nucleic Acids Res. 2018;46(2018):D1121-d1127.
47. Wang Y, Zhang S, Li F, Zhou Y, Zhang Y, Wang Z, Zhang R, Zhu J, Ren Y, Tan Y, Qin C, Li Y, Li X, Chen Y, Zhu F. Therapeutic target database 2020: enriched resource for facilitating research and early development of targeted therapeutics. Nucleic Acids Res. 2020;48:D1031-d1041.
48. Zhou Y, Zhang Y, Zhao D, Yu X, Shen X, Zhou Y, Wang S, Qiu Y, Chen Y, Zhu F. TTD: therapeutic target database describing target druggability information. Nucleic Acids Res. 2024;52:D1465-d1477.
49. Basar MA, Hosen MF, Kumar Paul B, Hasan MR, Shamim SM, Bhuyian T. Identification of drug and protein-protein interaction network among stress and depression: a bioinformatics approach. Inf Med Unlocked. 2023;37:101174.
50. Song P, Gao Z, Bao Y, Chen L, Huang Y, Liu Y, Dong Q, Wei X. Wnt/β-catenin signaling pathway in carcinogenesis and cancer therapy. J Hematol Oncol. 2024;17:46.
51. Vimalraj S, Hariprabu KNG, Rahaman M, Govindasami P, Perumal K, Sekaran S, Ganapathy D. Vascular endothelial growth factor-C and its receptor-3 signaling in tumorigenesis. 3 Biotech. 2023;13:326.
52. Rauniyar K, Jha SK, Jeltsch M. Biology of vascular endothelial growth factor C in the morphogenesis of lymphatic vessels. Front Bioeng Biotechnol. 2018. https://doi.org/10.3389/fbioe.2018.00007.
53. Mandriota SJ, Jussila L, Jeltsch M, Compagni A, Baetens D, Prevo R, Banerji S, Huarte J, Montesano R, Jackson DG, Orci L, Alitalo K, Christofori G, Pepper MS. Vascular endothelial growth factor-C-mediated lymphangiogenesis promotes tumour metastasis. EMBO J. 2001;20:672–82.
54. Yamaguchi R, Yano H, Nakashima O, Akiba J, Nishida N, Kurogi M, Kojiro M. Expression of vascular endothelial growth factor-C in human hepatocellular carcinoma. J Gastroenterol Hepatol. 2006;21:152–60.
55. Han W, Hou G, Liu L. Polyphyllin I (PPI) increased the sensitivity of hepatocellular carcinoma HepG2 cells to chemotherapy. Int J Clin Exp Med. 2015;8:20664–9.
56. Liu Y, Ren W, Bai Y, Wan L, Sun X, Liu Y, Xiong W, Zhang YY, Zhou L. Oxyresveratrol prevents murine H22 hepatocellular carcinoma growth and lymph node metastasis via inhibiting tumor angiogenesis and lymphangiogenesis. J Nat Med. 2018;72:481–92.
57. Thompson MD, Monga SP. WNT/beta-catenin signaling in liver health and disease. Hepatology. 2007;45:1298–305.
58. Cheng Z, Yuan X, Qu Y, Li X, Wu G, Li C, Zu X, Yang N, Ke X, Zhou J, Xie N, Xu X, Liu S, Shen Y, Li H, Zhang W. Bruceine D inhibits hepatocellular carcinoma growth by targeting β-catenin/jagged1 pathways. Cancer Lett. 2017;403:195–205.
59. Gao ZX, Zhang ZS, Qin J, Zhang MZ, Cao JL, Li YY, Wang MQ, Hou LL, Fang D, Xie SQ. Aucubin enhances the antitumor activity of cisplatin through the inhibition of PD-L1 expression in hepatocellular carcinoma. Phytomedicine. 2023;112: 154715.